Fabrication of ceramic cores via layered extrusion forming using graphite as pore-forming agent

Shiyan Tang, Li Yang, Guanjin Li, Xinwang Liu and Zitian Fan

Huazhong University of Science and Technology State Key Laboratory of Materials Processing and Die & Mould Technology, Wuhan, Hubei, China
Shiyan Tang d201477247@hust.edu.cn; Zitian Fan fanzt@hust.edu.cn

Abstract. Graphite powders were introduced in aqueous alumina paste to prepare alumina cores with high porosity using layered extrusion forming, which was a type of additive manufacturing methods. Rheological behaviours of pastes with different solid loading were tested. Paste composed of 50vol.% alumina loading and 5g graphite powders generated specimens with highest shape retention and finest surface quality. During formation and sintering process, basic shapes of rectangular specimens could be well maintained. With the increase of graphite addition, open porosity increased and flexural strength decreased of sintered specimens. Specimens prepared from paste with 50vol.% alumina loading and 10g graphite powders possessed best comprehensive performance, which was promising for application in alloys casting.

1 Introduction

Super alloys used for the aerospace area have the tendency of complex structure, which correspondingly requires the complex inner structures for the ceramic cores [1]. Conventionally, ceramic cores are prepared by gel casting, injection molding and hot-pressing injection, which involved the processing of complex metal or plastic molds and the adoption of toxic chemicals [2–4]. Thus, it is necessary to develop a practically available process for fabricating ceramic cores, which should be a low-cost, simple and effective approach.

As a rising technique, additive manufacturing has gained extensive attention because of its high efficiency and low waste [5]. Widely concerned additive manufacturing methods include 3D printing, stereolithography, laser selective sintering and layered extrusion forming [6–9]. Layered extrusion forming is now extended for ceramics formation, in which a controll system is employed to deposit aqueous ceramic pastes in a continuous fashion to produce complex-shaped specimens [10,11]. Layered extrusion forming adopts aqueous ceramic slurries to directly fabricate specimens, which eliminates nozzle jamming problem and is relatively low cost and high efficient. In previous researches, similar manufacturing methods have been used to develop biological scaffolds for controlled architecture and porosity [12,13]. Nowadays, in order to successfully apply layered extrusion forming into ceramic cores, the focus is to develop a suitable paste system. In layered extrusion forming processes pastes are generally highly solid loaded, which is typically comprising ceramic powders, dispersant and aqueous binder system [14]. To satisfy the requirements of ceramic core used in alloys casting, pore-forming agents are necessary in paste composition to generate high porosity. Commonly used pore-forming agents are materials that could be removed during sintering process, including starch, PMMA beads and graphite [15–17]. Among these pore-forming agents, graphite is water-insoluble and relatively low cost.

In this paper, we developed aqueous alumina paste composed of methylcellulose as binder and graphite as pore-forming agent. Pastes with different solid loadings were treated with rheological tests. Green specimens fabricated under working conditions with pastes of different solid loadings were compared. Specimens sintered at different temperature were tested for open porosity, flexural strength and microstructure.

2 Experimental procedures

2.1 Materials

Alumina powder (≥98wt.%, Qingdao Almatis Co., Ltd, China) with average diameter of 5.09 μm was used as received directly from the supplier without any treatment. Methylcellulose (≥99.5wt.%, Sinopharm Chemical Reagent Co., Ltd., China) was used as binder in the slurry composition. Graphite (≥99.95wt.%, Sigma-Aldrich, United States) with average size of 0.33 μm was adopted as pore former and acetic acid (≥99.5wt.%, Sinopharm Chemical Reagent Co., Ltd., China) was employed as dispersant.

2.2 Paste preparation and layered extrusion forming

Figure 1 shows the diagrammatic forming process. Premixed solution containing 2wt.% binder was prepared by dissolving MC in deionized water. The alumina particles were added to solution by mechanical mixing to form 46-52vol.% slurries. Ball mill mixing was carried to facilitate mixing in a planetary ball mill (QM-3SP2, NJU-YQ, Co. Ltd., China) with zirconia balls and polyethylene container for 9h at 270rpm.

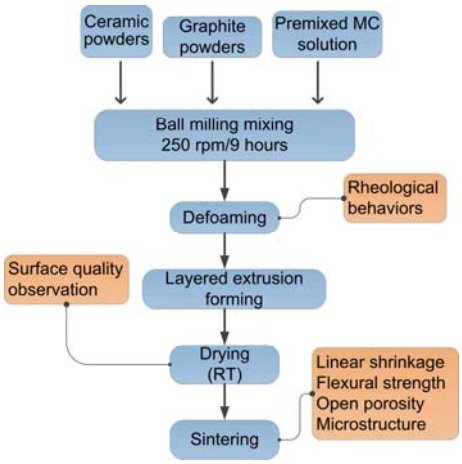

Figure 1 Detailed flowchart of layered extrusion forming

Figure 2 showed the device employed during the layered extrusion forming. The device consisted of three sections: a computer which built the structure and translated mobile paths into g-code, a 3D mobile platform which moved under the instructions of computer and an extrusion system which ejected slurry on demand and an air controller providing pressured air as driving force. The interrelated processing parameters were listed in Table 1.

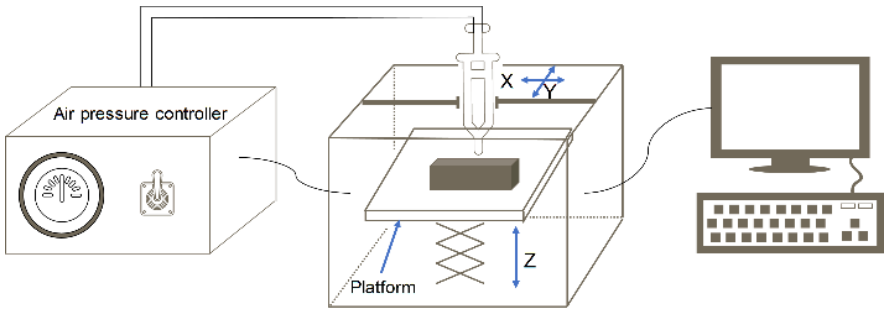

Figure 2 Self-developed device

Table 1 Parameters during layered extrusion forming process

Parameter	Value	Definition
Slice height	0.62mm	deposited layer height
Path speed	20mm/s	speed of syringe nozzle
Path width	1.00mm	deposited layer width
Gap	2mm	distance between nozzle and previously deposited layer

After formation, specimens were placed in ambient conditions for 24h until removal of extra water. Subsequently, the organic binder was removed at 600℃ for 60 minutes and then sintered at 1500℃ for 120 minutes to generate ceramic cores.

2.3 Characterizations

Rheological behaviours were tested on a rheometer (DHR-2, TA, USA), which adopted a parallel plate of 25 mm in diameter and a testing gap of 1000 μm. Viscosity was measured under the continuous shear mode from $1s^{-1}$ to $500s^{-1}$ at 25°C. Dimensional measurements were carried out to calculate the shrinkages of the sintered bodies. The Archimedes' method was taken to test the apparent porosity. Three-point-bending method was employed to measure the flexural strength (test bars: 50mm×10mm×5mm) on a high temperature permanent performance tester (AG-100KN, Shimadzu, Japan), which worked under the 40 mm spacing span and 0.05 mm/min punch displacement speed. Stereoscopic microscope (Stemi 508, Carl Zeiss, Germany) was employed to observe the surface images of green alumina specimens. Microstructures of sintered specimens were observed by scanning electron microscopy (Quanta200, FEI, The Netherlands).

3 Result and Discussion

Rheological behaviors of alumina-graphite paste with different solid loadings are shown in Figure 3. Viewing from Figure 3, the viscosity is increased with the increase of solid loading. The maximum shear rate for each paste during extrusion is calculated by Eq. (1):

$$\dot{\gamma} = \frac{4Q}{\pi r^3} \qquad (1)$$

where Q is volumetric flow rate and r is the radius of nozzle. When solid loading increases from 46 vol.% to 52 vol.%, calculated maximum shear rate is enhanced from 18.14 to $42.05s^{-1}$ and the nominal viscosity is increased from 0.44 to 23.21Pa·s with symbols marked in Figure 3. Pastes suitable for layered extrusion forming are supposed to be shear-thinning and to maintain shape during formation process, pastes should have high resistance to deformation. Paste with 46vol.% solid loading is not suitable for this formation process, for its poor shape retention and resistance to deformation.

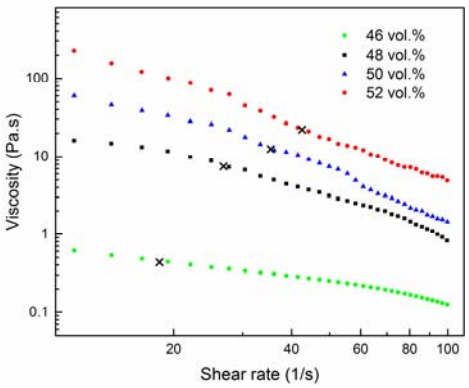

Figure 3 Flow behaviors of ceramic pastes with solid loadings varying from 46~52vol.%.

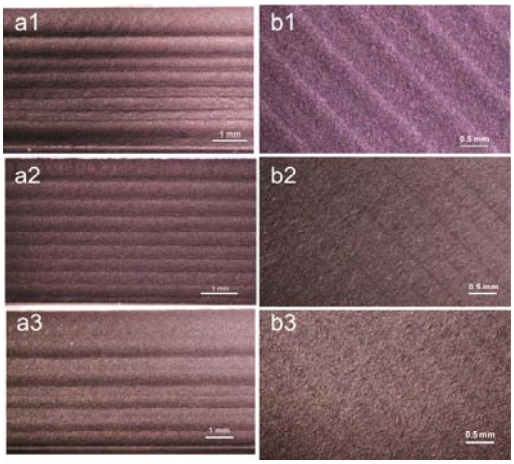

Figure 4 Surface images: (a) side surface quality and (b) top surface quality at different solid loadings: (1) 48vol.%; (2) 50vol.% and (3) 52vol.%.

Images of green specimens formed with 48 to 52vol.% solid loading plus additional 5g graphite are shown in Figure 4. Top surface of every specimen shows no pores or cracks. Viewing from Figure 4, specimens prepared with solid loading of 48vol.% and 52vol.% exhibits defects and flaws at side surfaces, while specimen fabricated with 50vol.% shows evenly distributed layer height and uniform surface morphology.

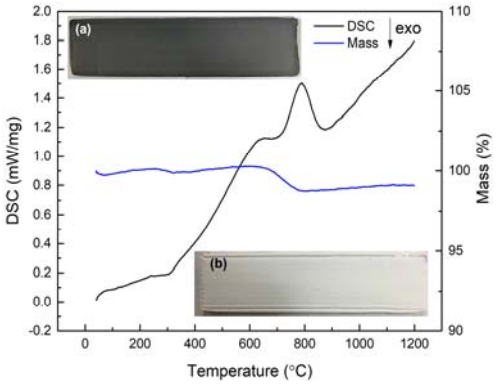

Figure 5 Thermal analysis: (a) green specimen and (b) specimen after sintering.

Green rectangular specimen is shown in Figure 5(a). After formation, basic shapes are well maintained. Based on the thermal analysis results, graphite oxidation reaction occurs between 700 and 900ºC. Sintered specimen is exhibited in Figure 5(b), which shows white appearance due to oxidation of graphite powders. No macro cracks or flaws are observed in surfaces due to slow heating rate.

Effect of the graphite powder addition on ceramic core properties is listed in Table 2. As the graphite powder addition increases, the linear shrinkage and pores formed increase correspondingly due to the oxidation reaction during sintering. According to previous research [15], the spherical-shaped pore structure can partially alleviate the stress concentration and contribute to the mechanical properties of ceramics defined by the Eq. (2)

$$\sigma = \sigma_0 exp(-nP) \qquad (2)$$

where P is the total porosity, σ_0 is the flexural strength when P is 0, n is the structural factor which is partly impacted by the spherical- shaped pore structure. However, the flexural strength of porous

ceramics is mainly dependent on the porosity. Thus, the flexural strength decreases evidently with increasing graphite powder content. According to the criteria for ceramic core [18], the open porosity should be more than 20% and maintain enough bending strength and in this study, the ceramic cores prepared with 50vol.% solid loading and additional 10g graphite powders possess the optimal comprehensive performances.

Table 2 Effect of graphite addition on mechanical properties

Paste composition	Linear shrinkage/%	Flexural strength/MPa	Open porosity/%
50vol.%+5g graphite	5.66	46.27	49.78
50vol.%+10g graphite	5.90	40.08	54.06
50vol.%+15g graphite	6.04	34.10	58.32

Microstructures of sintered specimens with paste composed of 50vol.% alumina with additional 10g graphite powders are shown in Figure 6. As shown in Figure 6 (a), there are no obvious cracks and defects. The upper surface is uniform and flat. During sintering process, binders are removed and graphite particles are oxidized, leaving pores inside the specimen. As shown in Figure 6 (b), alumina particles are bonded with each other and pores are left between particles. The same phenomenon is also observed in fracture microstructure.

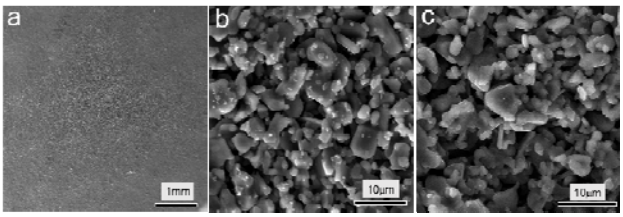

Figure 6 Microstructures of sintered specimens with paste composed of 50vol.% alumina plus 10g graphite powders: (a) general surface image; (b) microstructure at upper surface and (c). fracture microstructure.

4 Conclusions

Alumina cores using graphite particles as pore-forming agent were fabricated via layered extrusion forming, which was a type of additive manufacturing methods. Paste composed of 50vol.% of alumina loading and additional 5g graphite generated specimens with most uniform surface quality and highest shape retention. Shapes of green and sintered specimens could be well maintained by controlled slow heating rate. By increasing graphite addition, open porosity increased while flexural strength decreased after sintering. Specimens prepared from paste composed of 50vol.% alumina loading and 10g graphite powders exhibited optimal comprehensive performance, which was suitable for cores used in alloys casting. The corresponding microstructures showed porous morphology and alumina particles bonded with each other after sintering.

Acknowledgements

The authors would like to express appreciations to the National Natural Science Foundation of China (Grant No.51775204), the Innovation Fund of Huazhong University of Science and Technology (NO.2018JYCXJJ020) and the Analytical and Testing Centre, HUST.

References

[1] Kim Y H, Yeo J gu, Lee J S and Choi S C 2016 Influence of silicon carbide as a mineralizer on mechanical and thermal properties of silica-based ceramic cores *Ceram. Int.* **42** 14738–42
[2] Liu F, Fan Z, Liu X, He J and Li F 2016 Aqueous gel casting of water-soluble calcia-based ceramic core for investment casting using epoxy resin as a binder *Int. J. Adv. Manuf. Technol.* **86** 1235–42
[3] Gromada M, Adam Swieca, Kostecki M, Olszyna A and Cygan R 2015 Ceramic cores for turbine blades via injection moulding *J. Mater. Process. Technol.* **220** 107–12
[4] Cai K F, Nan C W, Schmuecker M and Mueller E 2003 Microstructure of hot-pressed B4C-TiB2 thermoelectric composites *J. Alloys Compd.* **350** 313–8
[5] Yang S and Zhao Y F 2015 Additive manufacturing-enabled design theory and methodology: a critical review *Int. J. Adv. Manuf. Technol.* **80** 327–42
[6] Hotta M, Shimamura A, Kondo N and Ohji T 2016 Powder layer manufacturing of alumina ceramics using water spray bonding *J. Ceram. Soc. Japan* **124** 750–2
[7] Wu H, Li D, Chen X, Sun B and Xu D 2010 Rapid casting of turbine blades with abnormal film cooling holes using integral ceramic casting molds *Int. J. Adv. Manuf. Technol.* **50** 13–9
[8] Tang H H and Yen H C 2015 Slurry-based additive manufacturing of ceramic parts by selective laser burn-out *J. Eur. Ceram. Soc.* **35** 981–7
[9] Tang S, Fan Z, Zhao H, Yang L, Liu F and Liu X 2018 Layered extrusion forming—a simple and green method for additive manufacturing ceramic core *Int. J. Adv. Manuf. Technol.*
[10] Moon Y W, Choi I J, Koh Y H and Kim H E 2015 Porous alumina ceramic scaffolds with biomimetic macro/micro-porous structure using three-dimensional (3-D) ceramic/camphene-based extrusion *Ceram. Int.* **41** 12371–7
[11] Costakis W J, Rueschhoff L M, Diaz-Cano A I, Youngblood J P and Trice R W 2016 Additive manufacturing of boron carbide via continuous filament direct ink writing of aqueous ceramic suspensions *J. Eur. Ceram. Soc.* **36** 3249–56
[12] Zhou K, Zhang X, Chen Z, Shi L and Li W 2015 Preparation and characterization of hydroxyapatite-sodium alginate scaffolds by extrusion freeforming *Ceram. Int.* **41** 14029–34
[13] Jo I H, Ahn M K, Moon Y W, Koh Y H and Kim H E 2014 Novel rapid direct deposition of ceramic paste for porous biphasic calcium phosphate (BCP) scaffolds with tightly controlled 3-D macrochannels *Ceram. Int.* **40** 11079–84
[14] Li Y Y, Li L T and Li B 2015 Direct ink writing of 3-3 piezoelectric composite *J. Alloys Compd.* **620** 125–8
[15] Wang F, Yin J, Yao D, Xia Y, Zuo K, Xu J and Zeng Y 2016 Fabrication of porous SiC ceramics through a modified gelcasting and solid state sintering *Mater. Sci. Eng. A* **654** 292–7
[16] Bai J 2010 Fabrication and properties of porous mullite ceramics from calcined carbonaceous kaolin and α-Al2O3 *Ceram. Int.* **36** 673–8
[17] Eom J-H, Kim Y-W, Song I-H and Kim H-D 2008 Processing and properties of polysiloxane-derived porous silicon carbide ceramics using hollow microspheres as templates *J. Eur. Ceram. Soc.* **28** 1029–35
[18] Qin Y and Pan W 2009 Effect of silica sol on the properties of alumina-based ceramic core composites *Mater. Sci. Eng. A* **508** 71–5